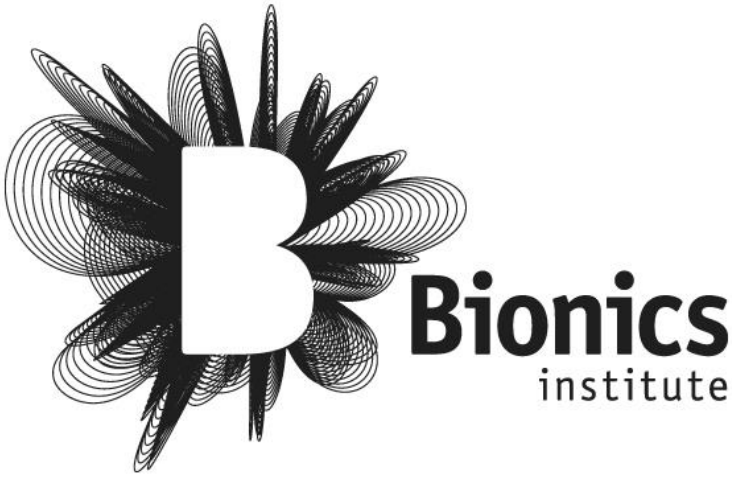

Manuscript published in J Neural Eng Revised: April 2014

Cortical activation following chronic passive implantation of a wide-field suprachoroidal retinal prosthesis

Joel Villalobos[1], **James B. Fallon**[1, 3], **David A.X. Nayagam**[1], **Mohit N. Shivdasani**[1,3], **Chi D. Luu**[2], **Penelope J. Allen**[2], **Robert K. Shepherd**[1, 3], **Chris E. Williams**[1, 3]

[1] Bionics Institute, East Melbourne VIC 3002, Australia

[2] Centre for Eye Research Australia, University of Melbourne, Royal Victorian Eye & Ear Hospital, East Melbourne, VIC 3002, Australia

[3] Medical Bionics Department, The University of Melbourne, VIC 3002, Australia

Corresponding Author:
Assoc. Prof. Chris E. Williams
Bionics Institute
384-388 Albert St
East Melbourne, VIC 3002, AUSTRALIA
Tel. +61 3 9288 3523, Fax +61 3 9288 2998
Email: cwilliams@bionicsinstitute.org

Abstract

Objective: The research goal is to develop a wide-field retinal stimulating array for prosthetic vision. This study aimed to evaluate the efficacy of a suprachoroidal electrode array in evoking visual cortex activity after long term implantation.

Approach: A planar silicone based electrode array (8 mm × 19 mm) was implanted into the suprachoroidal space in cats (n_{total} = 10). It consisted of 20 platinum stimulating electrodes (600 μm diameter) and a trans-scleral cable terminated in a subcutaneous connector. Three months after implantation ($n_{chronic}$ = 6), or immediately after implantation (n_{acute} = 4), an electrophysiological study was performed. Electrode

total impedance was measured from voltage transients using 500μs, 1mA pulses. Electrically evoked potentials and multi-unit activity were recorded from the visual cortex in response to monopolar retinal stimulation. Dynamic range and cortical activation spread were calculated from the multi-unit recordings.

Results: The mean electrode total impedance *in vivo* following 3 months was 12.5±0.3 kΩ. Electrically-evoked potentials were recorded for 98% of the electrodes. The median evoked potential threshold was 150 nC (charge density 53 μC/cm^2). The lowest stimulation thresholds were found proximal to the *area centralis*. Mean thresholds from multiunit activity were lower for chronic (181±14 nC) compared to acute (322±20 nC) electrodes ($P < 0.001$), but there was no difference in dynamic range or cortical activation spread.

Significance: Suprachoroidal stimulation threshold was lower in chronic than acute implantation and was within safe charge limits for platinum. Electrode-tissue impedance following chronic implantation was higher, indicating the need for sufficient compliance voltage (e.g. 12.8V for mean impedance, threshold and dynamic range). The wide-field suprachoroidal array reliably activated the retina after chronic implantation.

Keywords: blindness, retinal prosthesis, suprachoroidal, electrical stimulation

1. Introduction

Visual prostheses have emerged as a viable treatment for blind patients who suffer retinal degenerative diseases [1]. Retinitis pigmentosa is one of the leading inherited causes of blindness in many countries and its symptoms include a progressive reduction of the visual field which increasingly impedes mobility [2]. Psychophysical studies have found that visual field size and contrast sensitivity correlate well with the level of orientation and mobility in retinitis pigmentosa (RP) patients [3, 4]. A therapeutic device aimed to assist with navigational tasks should provide a minimum visual field of 10–15˚ [5]. Electrical stimulation of the degenerated retina has been shown to be a feasible way of restoring visual perception [6-8]. Possible treatment alternatives also include gene therapy, stem cell therapy and retinal transplantation, but these have not translated into consistent clinical outcomes to date [9]. Clinical trials with retinal prostheses, however, have shown that blind patients can perceive some patterns and orientations [10-12], and a prosthesis from Second Sight Medical Products Inc. has recently been approved by the US Food and Drug Administration.

Retinal prostheses have been successful at producing visual percepts in animal models and have been placed in several anatomical locations in the eye; i.e., epiretinal, subretinal, suprachoroidal, intrascleral and extraocular. Epiretinal and subretinal placement of electrode arrays have had the lowest thresholds for electrical stimulation of the retina [13-16] and have been successful in clinical trials. However, implanting a wide visual prosthesis (more than 20˚ of visual field) using these approaches is challenging due to the limitations in implant size that can be placed subretinally [17] or due to mechanical instability associated with epiretinal implantation [18, 19]. In contrast, evaluation of extraocular stimulation demonstrated high thresholds with a wide area of retinal activation [6, 20]. Suprachoroidal and intrascleral stimulation sites provide a good compromise with higher thresholds (compared to epiretinal and subretinal) [21-23] but punctate retinal activation [24] and access for safe surgical implantation of larger planar electrode arrays [25].

Biocompatibility of suprachoroidal electrode arrays has been studied with promising results [26, 27]. However, to date there has been no investigation on the effect of chronic implantation on the efficacy of retinal stimulation from the suprachoroidal space. We previously reported that a thin fibrous

capsule and mild foreign body response formed around the suprachoroidal electrode array after 3 months of implantation [28]. The present study characterized the efficacy of a large-format suprachoroidal electrode array to evoke punctate activity in the visual cortex following 3 months of implantation. Further, this study assessed the effect of chronic implantation by comparing cortical responses between chronic and acute implantation.

2. Materials and Methods

These procedures were approved by the Animal Research Ethics Committee of the Royal Victorian Eye & Ear Hospital. The procedures complied with the "Australian code of practice for the care and use of animals for scientific purposes" (7th edition 2004), the "Principles of laboratory animal care" (NIH publication No. 85-23, revised 1985) and the Australian "Prevention of cruelty to animals act" (1986 and amendments). The animals were bred and housed by the Biological Research Centre in the Royal Victorian Eye & Ear Hospital. Ten normally sighted adult cats weighing 2.7–5.5 kg were implanted with a suprachoroidal electrode array in the left eye. Six of these were implanted chronically. After 3 months of implantation, the animals were anesthetized for an electrophysiological experiment lasting 2 days. Four control animals underwent identical surgical implantation, followed immediately by acute electrophysiology where multi-unit activity was recorded.

2.1. Suprachoroidal electrode array

An electrode array was fabricated in a 19 mm × 8 mm biocompatible silicone substrate. The array consisted of 20 electrodes (plus 1 unconnected) made of platinum (Pt), spaced 1 mm from center to center. The array is shown in figure 1. In a human eye, the visual field coverage would be approximately 9˚ × 20˚ [29], while in the cat eye it was approximately 11˚ × 24˚ [30]. The electrodes were 600 μm in diameter to allow for an increase in total impedance with chronic implantation and because brightness matching at suprathreshold levels appears to be more efficient with relatively large electrodes [31]. The 1 mm electrode pitch was used because the minimum two point distance for perceptual discrimination was in the range of 0.6–1.7 mm for epiretinal studies [32]. Two return electrodes (Pt, ⌀ 2 mm) were placed within the substrate body. It has been established that there is no

significant difference in monopolar stimulation thresholds with suprachoroidal versus vitreous return electrodes [33-35], while suprachoroidal implantation has less associated risks. The implant substrate had a maximum thickness of 1 mm and minimum of 150 μm. This was built with layers of silicone sheet (Dow Corning) and silicone adhesive (MED-1137; Nusil). The top surface was contoured (figure 1A) to provide an anatomical fit and an even distribution of pressure onto the spherical sclera.

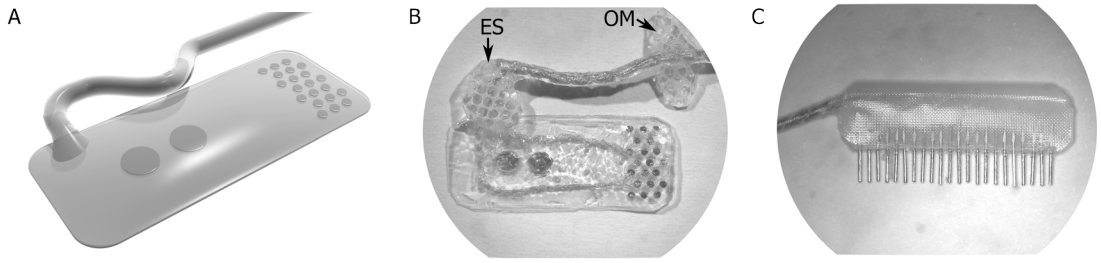

Figure 1. Suprachoroidal wide-field electrode array. A: Schematic of the contoured implant substrate optimized for insertion into the suprachoroidal space. B: Electrode array used in this study with 21 stimulating electrodes and 2 return electrodes made of Pt in a silicone elastomer substrate and connected to a helical cable, with episcleral (ES) and orbital margin (OM) attachment points. C: Connector at the end of the cable made of Pt and silicone elastomer for chronic subdermal implantation.

There were 22 Pt-Ir (90-10%, ⌀ 25 μm; Sigmund Cohn) wires attached to the electrodes via spot welding and these were assembled into a helical cable lead. The cable traversed the sclera at one edge of the incision site. An episcleral patch made of silicone and reinforced with polyester mesh (figure 1B) was used to cover the trans-scleral exit point and provide fixation for the cable lead. A similar reinforced silicone patch was used to fix the cable to the orbital margin. The wires terminated in a biocompatible connector designed to be implanted subcutaneously (figure 1C). Baseline electrode total impedance was measured in normal saline prior to implantation. The electrode arrays were cleaned in consecutive baths of detergent (Pyroneg; JohnsonDiversey), ethanol, isopropanol, distilled water and then autoclaved at 121 °C for 30 min.

2.2. Surgical implantation

The cats were induced into anesthesia with a dose of xylazine (1 mg/kg, subcutaneous (s.c.); Xylazil; Troy Labs, Australia) and ketamine (10 mg/kg, intramuscular (i.m.); Ketamil; Troy Labs) [36]. An endotracheal tube was inserted and anesthesia maintained with a continuous flow of isoflurane

(Delvet, Australia) and oxygen during surgery. Heart rate, respiration rate, end-tidal CO_2, blood pressure and core body temperature were monitored and anesthetic adjusted to maintain these within normal levels (170–220 beats per minute, 10–20 breaths per minute, 3–5 % CO_2, 130/100 −160/120 mmHg and 36–38 °C). Paw withdrawal reflex was also tested to monitor appropriate anesthetic level. Fluid replacement was provided by s.c. bolus of compound sodium lactate solution (2.5 ml/kg/hr; Hartmann's; Baxter). For chronic implantation, the animal was given amoxicillin-clavulanate suspension once daily (10mg/kg, s.c; Clavulox; Pfizer, Italy) during the first week postoperative. Topical applications of prednisolone (Prednefrin Forte; Australia), atropine (Atropt; Sigma Pharmaceuticals, Australia) and chloramphenicol (Chlorsig; Sigma Pharmaceuticals) were administered twice daily postoperatively and tapered off as required.

The surgical procedure was developed during acute studies with a thin film array [25] and refined to allow strong scleral closure for chronic implantation [28]. In brief, a full-depth scleral incision (9 mm long) was performed at 5 mm from the limbus in the temporal quadrant. A suprachoroidal pocket was dissected using a Crescent blade. The electrode array was then inserted into the suprachoroidal space and advanced 17 mm towards the posterior pole to position it beneath the *area centralis*. The scleral wound was closed with nylon sutures (Ethicon; Johnson & Johnson, Australia) and the episcleral patch was sutured on top of the trans-scleral cable exit. The cable lead was directed posteriorly and then the second patch sutured onto the zygomatic process. The implantable connector at the end of the cable was implanted subcutaneously. The eye fundus was inspected with a quadraspheric lens (Volk Optical, Mentor, OH, USA). Immediately postoperatively the eye was visually assessed for surgical trauma and electrode array location. For chronic implantation, fundus assessments were performed daily postoperatively for 7 days (with indirect ophthalmoscope), then at 2 weeks (under anesthesia, ketamine-xylazine, 10 mg/kg – 1 mg/kg, s.c.) and then again at 3 months during the stimulation experiment.

2.3. Animal preparation for stimulation

At the end of the 3 month implantation period (chronic cohort), or following acute implantation (control cohort), the animals were prepared for a retinal stimulation and cortical recording experiment

lasting 2 days. In chronically implanted animals, anesthesia was induced with ketamine-xylazine (10 mg/kg and 1 mg/kg respectively, s.c.). Anesthesia was maintained throughout the experiment with an intravenous (i.v.) flow of sodium pentobarbital (Pentobarbitone) at a variable rate (loading dose 6 mg/hr, maintenance dose titrated to maintain normal physiological parameters). Physiological parameters and withdrawal reflex (as detailed above) were used to monitor and maintain anesthesia level. Fluid replacement was provided by i.v. infusion of compound sodium lactate solution (2.5 ml/kg/hr; Hartmann's, Baxter). Daily doses of Clavulox (3.5 mg/kg, s.c.) and dexamethasone (0.1 mg/kg, i.m.; Dexason) were administered as antibiotic and for the prophylaxis of brain edema respectively.

The subcutaneous connector was extracted and the skin closed with cyanoacrylate glue. A tracheotomy was performed and an endotracheal tube inserted. The physiological parameters were monitored, for the duration of the experiment, using a capnograph and sphygmomanometer (Cardell; Sharn Veterinary) positioned on the tracheotomy tube and hind leg, respectively. The animals were placed in a stereotaxic frame (David Kopf Instruments, Tujunga, CA). To expose the visual cortex bilaterally, a craniotomy was performed from 5 mm caudal to 15 mm rostral of the inter-aural line and 6 mm lateral towards both sides of the midline.

At the end of the experiment the animals were terminated with an overdose of sodium pentobarbital (150 mg/kg, i.v.; Pentobarbitone). After perfusion with neutral buffered formalin, the eyes were collected for histopathological assessment; these results were presented in a previous publication [28].

2.4. Electrical stimulation

The retina was stimulated with the suprachoroidal electrodes using monopolar, constant-current, symmetric, biphasic pulses with a leading cathodic phase. Each phase was 500 μs in duration and there was an inter-phase delay of 25 μs. The stimuli were presented at a rate of 1.5 pulses per second which does not result in attenuation of the elicited response for repetitive retinal stimulation [37]. The charge injection density was kept below 180 $\mu C/cm^2$, which is within the widely accepted non-gassing limits for Pt with wide pulses [38]. Electrodes were stimulated with a monopolar return configuration using

one of the suprachoroidal return discs from the array. They were shorted to the return electrode after each stimulus pulse. The custom built stimulator had a compliance voltage of 24 V. The stimulator output was connected to the individual electrodes using an automated switching system [39]. Impedance was calculated using the voltage transient [40] measured during the application of a monopolar constant current biphasic pulse to each electrode of 1 mA and 500 µs (figure 2) as has been described in [41]. Briefly, the voltage transient was defined to have an access voltage (Va) and a polarization voltage (Vp). These arise from the electrode-tissue interface's access resistance (Ra) and polarization impedance (Zp). Total impedance (Zt = Ra + Zp) was defined as the peak voltage in the leading cathodic phase divided by the measured current output (Zt = Vt / It). The baseline electrode impedance was measured initially in saline at room temperature. *In vivo* total impedance was then measured in chronically implanted animals, after 3 months of implantation, and in acutely implanted controls.

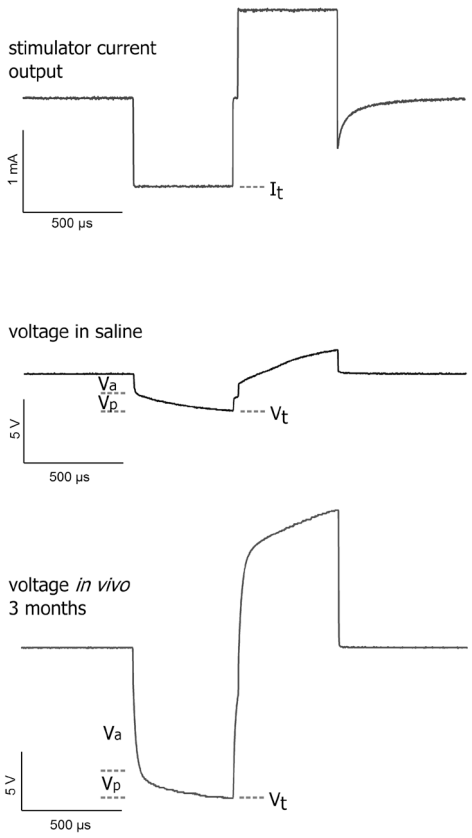

Figure 2. Stimulation biphasic current pulse and electrode voltage waveforms recorded during impedance measurements. Total impedance (Z_t) was calculated from maximum voltage (V_t) and output current (I_t): $Z_t = (V_a + V_p) / I_t = V_t / I_t$

2.5. Electrically evoked cortical recordings

A platinum ball macro-electrode (3 mm diameter) was placed on the dura over the visual cortex to record electrically evoked potentials (EEPs) in the six chronically implanted animals. The recording electrode was placed in the midline, between the posterior lateral gyri [42]. A platinum needle was placed in the neck as reference and an electrode in the thorax was used as a ground. Cortical potentials were recorded using a bioamplifier (ISO-80; World Precision Instruments) and an acquisition module (NI USB-6251; National Instruments). Recordings were performed in 2 independent consecutive sets of 50 averaged repetitions. Waveforms were filtered for a band-pass of 10–2000 Hz. The input-output function per retinal electrode was calculated using stimulus current levels ranging from 0 to 975 μA in steps of 75 μA, as shown in figure 3A. The current levels were presented in random order and analyzed using custom scripts in IgorPro software (Wavemetrics). EEP threshold [34] was considered as the minimum stimulus current level that yielded monotonically increasing peaks of at least 0.3 mV, within 30 ms of the stimulus (figure 3B). These peaks had to be aligned on the 2 sets of the stimulation function. The EEP waveforms were verified to contain the typical short-latency positive and shallow negative components corresponding to early electrically evoked activity, as has been described in previous publications [34, 43]. EEP recordings were not performed systematically in the acutely implanted control animals.

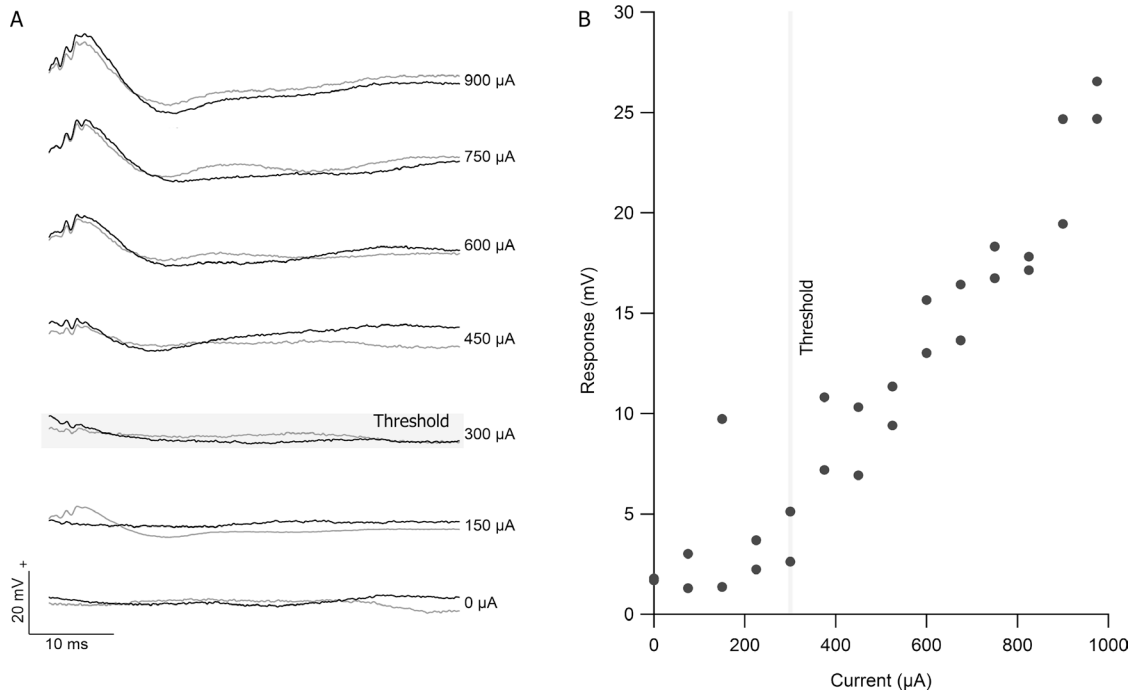

Figure 3. Electrically evoked cortical potentials recorded from stimulation of a single suprachoroidal electrode. A: cortical traces recorded epidurally over visual cortex at different stimulating current levels, averaged over 50 repetitions; black trace is first set and gray is second set; initial 2 ms not shown due to suppression of artifact. B: input-output function of the EEP response amplitude (within 20 ms) vs. stimulus amplitude; threshold was defined as the start of monotonically increasing peaks.

To assess the effect of electrode location with respect to the retina, the outlines of the electrode arrays were obtained from fundus images of the chronically implanted animals. Figure 5A illustrates the approximate locations. The implant was typically placed beneath the superior retina where the lower corner of the implant was visible above the horizontal meridian (HM). Due to projection distortion in the fundus images, the implant locations were grouped categorically according to anatomical landmarks. The experiments were categorized in 3 groups according to the location of the lower corner relative to the HM (calculated in optic-disc diameters): I, implant corner inferior to HM; II, implant 1-2 disc diameters superior to the HM; III, implant more than 3 disc diameters superior to the HM. The electrode arrays had 7 rows of 3 electrodes. The analysis was therefore limited to vertical electrode location according to the electrode row position within the array, where the rows were numbered 1 to 7 starting from the bottom. An additive adjustment to the electrode row number was defined for each experiment (i.e. -4, -1, 2) to normalize the vertical location with respect to the horizontal meridian.

The arbitrary adjustment was related to the ratio of distance between electrode rows (0.87 mm) and the size of the optic disc (approximately 1 mm).

2.6. Multiunit activity cortical recordings

A 60 channel recording electrode array (Blackrock Microsystems, Foxborough, MA) was implanted in the visual cortex contralateral to the implanted eye to record evoked multiunit activity. The array was located 6 mm rostral from the inter-aural line and 1 mm lateral from the midline. Multiunit recordings were obtained from six chronically implanted animals and four acutely implanted controls. The needle-shaped recording electrodes had a platinum surface with a nominal impedance of ~400 kΩ at 1 kHz, in an array configuration of 6 × 10 electrodes with 400 μm pitch. These Utah intracortical microelectrode arrays are designed for recording in cortex [44]. The electrode arrays covered an area of 2 mm × 3.6 mm and penetrated into the cortex approximately 1 mm, chosen to target neurons in layer 4C. A Cerebus recording system (Blackrock Microsystems, Foxborough, MA, USA) was used to record multiunit activity with a sampling rate of 30 kHz. Input-output functions were calculated from stimulating the suprachoroidal electrodes with 10 stimulus pulses per level over a range of 0–975 μA, in 25 μA steps, presented in random order. Offline processing with custom scripts was used to identify spikes, as was published previously [45, 46]. Briefly, the stimulation artifact was suppressed and the spikes on the filtered signal (0.3–5 kHz Butterworth band-pass) that exceeded 4 times the root-mean-square of the signal, over a moving 60 s window, were counted within a window of 3–20 ms post-stimulus onset (figure 4A).

To determine threshold and dynamic range, sigmoid curves were fitted to the spiking response to stimulus amplitude (figure 4B). The current level at 50% (P50) of the saturation spike count was defined to be the threshold, since it corresponded to the steepest slope in the response curve [36]. The dynamic range was calculated as the logarithmic ratio (dB) between the currents evoking 90% and 10% (P90 and P10) of the saturating neural activity. For each suprachoroidal electrode stimulated, only the cortical recording electrode with the best response (lowest P50 threshold) was used for analysis of threshold and dynamic range.

To quantify the selectivity of stimulation in the cortical response, the spiking activity across the recording array was expressed as a function of the distance to the recording electrode with the lowest threshold. A stimulation level of P90 (near saturation) of the recording electrode with the lowest threshold was chosen to calculate the spread of cortical activation. An exponential decay function was then fitted to this spatial response and the inverse decay constant $1/\tau$ was used as a measure of cortical selectivity [45].

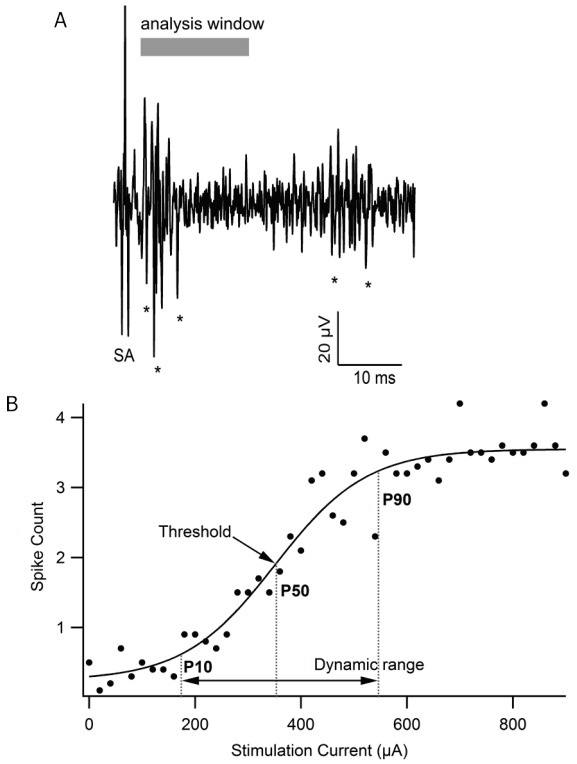

Figure 4. Example of multiunit activity in the visual cortex in response to stimulation of a suprachoroidal electrode. A: Trace of a cortical recording following a monopolar stimulation pulse in the retina where the stimulus artifact (SA) and post-stimulus spiking (*) are visible; the spikes occurring within a window of 3–20 ms after stimulus onset were counted during analysis. B: Plot of multiunit spike response for a cortical / suprachoroidal electrode pair over a range of stimulus current levels, showing sigmoidal function fit with corresponding threshold (P50) and dynamic range (P90 - P10).

2.7. Statistical analyses

Minitab 16 was used for the statistical analyses. Results are presented at a double-tailed, 5% significance level. Population distribution locations are represented with mean ± standard error (SE); or in the case of skewed distributions the median and 95% confidence interval (CI) for the median are given. Pearson correlation was used for testing associations. Total impedance data were compared

using paired T-tests where pairing was individual electrodes. Variability of the total impedance distributions was tested using F tests for equal variances. Effect of electrode location on the EEP threshold distribution was tested with non-parametric analysis using a Kruskal-Wallis test. Distributions of multi-unit activity data were compared with Student's *t*-test.

3. Results

The implant was stable in all chronically implanted animals and there was a thin fibrous tissue capsule on the electrode array surface [28]. Before implantation each array had 18 to 20 functional electrodes, not short or open circuited, for a total of 113 electrodes across 6 chronic implants. Following 3 months of implantation, there were $N = 103$ functional electrodes (91%) and each implant had 16 to 19 functional electrodes.

3.1. Electrode Impedances

The average total electrode impedance measured *in vivo* after 3 months of implantation was 12.5 ± 0.3 kΩ (mean ± SE). The *in vivo* total electrode impedance was higher than the baseline measured in saline before implantation of 3.13 ± 0.04 kΩ (paired T-test: $T = -31.4$, $P < 0.001$). The increase in total impedance for each electrode from baseline to *in vivo* was higher for chronically implanted electrodes (Z_t *in vivo* / Z_t baseline = 416 %) than for acute controls (322 %) (T-test: $T = -7.16$, $P < 0.001$). Impedance measurements were repeated on the second day of the electrophysiology experiment, after the electrodes had been repeatedly stimulated. The mean total impedance after stimulation was 10.8 ± 0.2 kΩ, which was 13 % lower than the initial *in vivo* total impedance (paired T-test: $T = 13.6$, $P < 0.001$). The range of *in vivo* total electrode impedance that includes 90% of the electrodes was 7.2–15.8 kΩ (5^{th} –95^{th} percentile).

3.2. Electrically evoked cortical potentials

Table 1. EEP thresholds and electrode impedances per experimental animal.

Subject No.	C3	C4	C5	C6	C7	C8
Median EEP threshold (density)	188	113	281	188	150	150

(nC ($\mu C/cm^2$))	(66.3)	(39.8)	(99.5)	(66.3)	(53.1)	(53.1)
Lowest EEP threshold (nC)	75	75	150	113	75	75
Mean electrode total impedance (kΩ)	11.3	12.8	11.7	11.1	11.3	7.4
Responsive / functional electrodes	18 / 18	16 / 16	16 / 18	16 / 16	13[a] / 16	19 / 19

[a] Three of the functional electrodes were not stimulated

Using monopolar stimulation, EEPs were successfully recorded for 98 out of the 100 electrodes tested, within the charge density limit of 180 $\mu C/cm^2$. The mean EEP threshold was 189 ± 9.8 nC/phase (charge density of 66.7 ± 3.5 $\mu C/cm^2$). The recorded positive peaks had a latency of 8–10 ms as shown in figure 3A. The distribution of the EEP thresholds had positive skewness of 1.21 and therefore the median was a more suitable descriptor. The median threshold was 150 nC/phase (53.1 $\mu C/cm^2$) with a 95% CI for the median of 150–188 nC/phase (53.1–66.3 $\mu C/cm^2$). The median threshold observed per experiment is presented in table 1. The lowest EEP threshold in a single animal was typically 75 nC/phase. The thresholds were different between animals (Kruskal-Wallis: $H = 40$, $P < 0.001$); but as expected from constant current stimulation, they were not found to be correlated with the *in vivo* total impedance (Pearson's $r = 0.19$).

The effect of threshold with respect to electrode locations on the retina was assessed. From the approximate implant locations in figure 5A, an additive adjustment to the electrode row number was defined for each experiment (table 2) to normalize the location with respect to the horizontal meridian. With the adjustment, an approximate coverage of 13 electrode rows (about 48˚ of visual field) was estimated across animals. Figure 5 shows the EEP thresholds per adjusted row across all experiments. There was a marked variation of the EEP threshold with the electrode location where the lower thresholds were in the central rows (central 7 rows vs. 6 peripheral rows, Mann-Whitney: $W = 2315$, $P < 0.0001$).

Table 2. Adjustment of electrode row according to the categorical grouping of implant location in each animal (figure 5A)

Subject No.	Approximate implant lower edge location	Electrode row adjustment

C3	1 – 2 DD sup. to HM	-1
C4	1 – 2 DD sup. to HM	-1
C5	> 3 DD sup. to HM	+1
C6	> 3 DD sup. to HM	+1
C7	1 – 2 DD sup. to HM	-1
C8	2 DD inf. to HM	-4

DD = (optic) disc diameters, HM = horizontal meridian

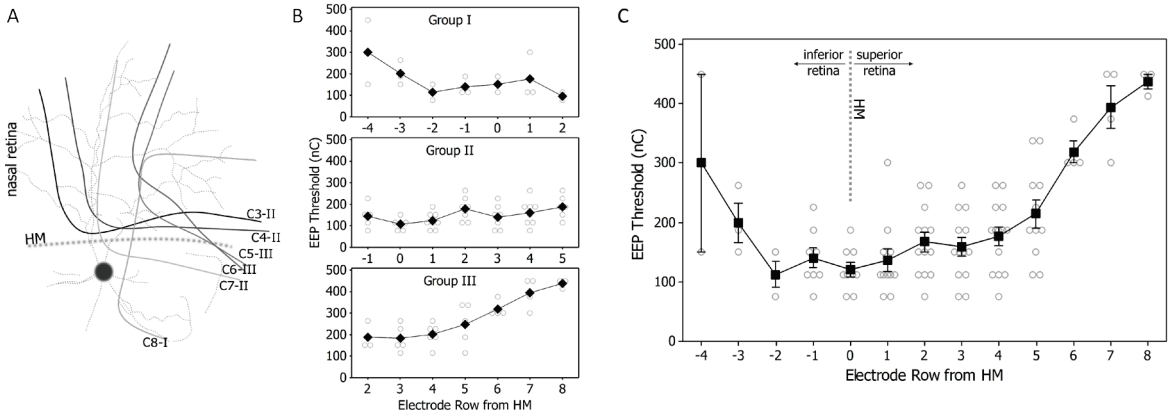

Figure 5. EEP thresholds per adjusted electrode row according to the categorical offset assigned in table 2. A: Approximate location of suprachoroidal implant outlines from fundus images, with respect to the optic disc (dark circle) and horizontal meridian (HM). Animal numbers and categorical groups are indicated on the solid lines representing the implant locations beneath the dotted exemplary retinal vessels. B: Threshold vs. electrode row trends per categorical group centered on HM. C: The aggregate of the data shows a vertical retinotopic distribution of EEP thresholds. Squares are mean, bars are standard error and circles are individual values.

3.3. Multiunit activity

From recordings of multiunit activity in the visual cortex, following electrical stimulation of the chronically implanted suprachoroidal electrodes, a P50 threshold was successfully obtained, in at least one cortical site, for 35 stimulated electrodes. These successful recordings were obtained with 4 animals (subjects C4, C5, C7 and C8). The mean stimulation charge for the P50 threshold was 181 ± 14 nC/phase, corresponding to a charge density of 64 ± 5 μC/cm^2, using the best cortical site per electrode (that which needed the least current to reach the 50% threshold). Recordings were not attempted in one animal (C3) and were unsuccessful in another (C6) likely due to change in recording site (anteriorly) because of cortical vasculature.

These multi-unit activity recordings in chronically implanted animals were compared to those from the acutely implanted control animals. There were 45 electrodes in these acutely implanted control animals for which a P50 threshold could be determined from cortical recordings. Figure 6A and figure 6B show that the mean threshold from the acutely implanted control electrodes was 80% higher than the chronically implanted ones (Student's t-test: $T = 5.74$, $P < 0.001$). However, the dynamic range (difference between P10 and P90 in a decibel scale) was not found to be different between chronic and acute electrodes as shown in figure 6C. The selectivity in cortical activation from electrical stimulation was not found to be different between chronic and acutely implanted electrodes (figure 6D).

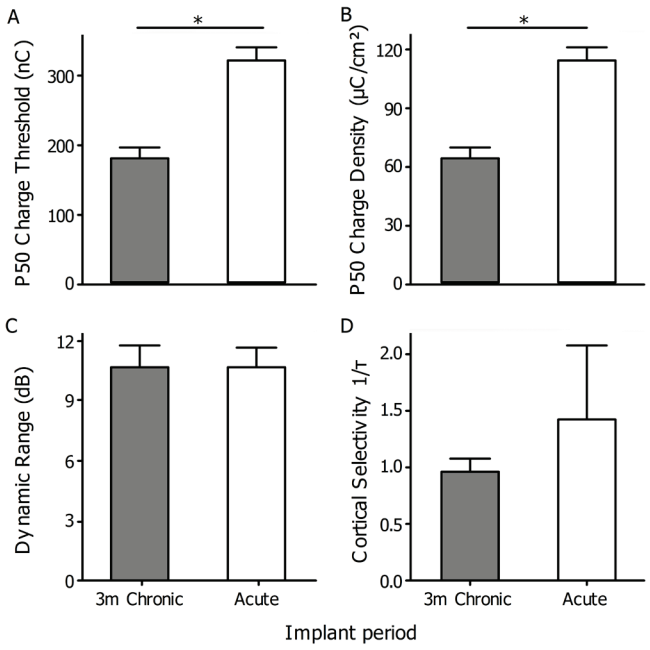

Figure 6. Comparison of multiunit cortical activity driven by monopolar electrical stimulation in chronically vs. acutely implanted suprachoroidal electrodes. A: The charge per phase and B: charge density required for activation of cortical units with 50% success (P50) were significantly lower in 3-month implantation compared with acute implants. C: Neither the dynamic range (difference of P90 and P10 in a decibel scale), D: nor the spatial selectivity of cortical activation (given by the inverse exponential fit parameter) differed significantly between chronic and acutely implanted electrodes. Bars represent mean and error bars are standard error. Stars represent statistically significant difference (*t*-test $P < 0.001$).

4. Discussion

The chronically-implanted suprachoroidal electrode array reliably evoked responses in the visual cortex with monopolar stimulation of single electrodes in 98 of 100 stimulated electrodes, well within safe electrochemical gassing limits for platinum. The electrode array and helical lead-wire [47]

showed reasonable durability (10 of 103 electrodes failed) after 3 months of implantation. Electrode arrays implanted in the suprachoroidal space have been found to be safe, mechanically stable [28] and to elicit cortical activity following acute implantation [34, 48, 49]. EEP thresholds reported from acute implantation are in the range of 26–200 nC [21, 22, 24, 34, 49] which is one order of magnitude higher than those for subretinal or epiretinal stimulation [14, 15, 21, 50]. This study is the first systematic report of thresholds from single electrode stimulation in chronically implanted suprachoroidal arrays. Comparison of multiunit activity between chronic and acute suprachoroidal implantation indicated a reduced threshold after chronic implantation, but no change in the dynamic range of stimulation. This suggests that chronic implantation of the electrode array has not damaged the neural targets for the stimulation. The higher thresholds found in acute implantation were presumably associated with an increase in distance between the electrode and the retina as a result of acute bleeding and edema [25]. This contrasts with the thin fibrous tissue encapsulation observed after 3 months of implantation [28]. The stimulation thresholds in this study do not greatly differ from those reported previously for acute suprachoroidal or intrascleral implantation [22, 34]. Importantly, the charge required to reach threshold is well within the traditionally accepted safe electrochemical injection limits for platinum electrodes [38, 51]. The selectivity in cortical activation from electrical stimulation was not found to be different between chronic and acutely implanted electrodes (figure 6D); but it was wider than the cortical selectivity reported previously with stimulation of 400 μm diameter electrodes [45]. This implies that the electric fields of the stimuli are reasonably localized on the retina and the fibrous tissue encapsulation does not have a substantial effect. Regarding stimulation-induced neural injury [52], further evaluation is required using long term supra-threshold stimuli to assess the safety of electrical stimulation on the retina.

The EEPs observed in the visual cortex indicated that the retinal stimulation was to some extent localized (figure 5). The thresholds seemed to correspond with the vertical location on the retina and the electrodes near the horizontal meridian had the lowest thresholds. This could be explained by variation of the visual field mapping of the cortical recording electrode and the exponential decrease in ganglion cell density with eccentricity [53]. The thresholds near area centralis and the similarities with

those in acute implantation [34] suggest that the chronic tissue reaction did not effect the efficacy of neural stimulation.

The observed short latency of the EEP and early spikes in the multi-unit responses are thought to relate to the direct response of retinal ganglion cells to electrical stimulation [43], since the responses of the outer retinal and bipolar cells typically have longer latencies [54]. A similar oscillatory response to the one observed early on the rise of the positive peaks, has been previously described from *in vitro* studies as nerve fiber activity and reverberation in the inner plexiform layer due to simultaneous excitatory and inhibitory inputs to the ganglion cells [55, 56].

The high *in vivo* electrode impedance, measured following 3 months of implantation, is linked with the good biocompatibility exhibited by the implant [28]. Tight fibroblast layers result in higher impedance than loose fibroblast layers and ongoing inflammation resulting from a foreign body reaction [57, 58]. The 3 month implantation period was considered sufficient to reach a steady scar response in the eye [59]. The drop in electrode impedance observed after electrical stimulation has been reported previously and is likely related to localized changes in the tissue adjacent to the electrode [41]. However, the relatively high total impedances indicate that relatively large surface area electrodes are required to reduce stimulator voltage requirements.

Epiretinal and subretinal implantation have been successful in clinical trials [10, 60, 61]. These devices are positioned closer to the target neural elements and have been expected to have a greater likelihood of eliciting high-acuity perception. However, addressing a large visual field can be challenging with epiretinal and subretinal techniques due to device size restrictions. The present efficacy results, combined with the simplicity of the suprachoroidal surgery [28], indicate that this approach is capable of providing effective stimulation over a range of more than 40˚ of visual field (figure 5A). As such, suprachoroidal arrays are a promising alternative for use in a safe, wide-field prosthesis, which is expected to be a useful mobility aid for late-stage RP patients.

Acknowledgements

The authors wish to thank Mark McCombe for assistance with surgeries; Helen Feng for implant manufacturing; Alexia Saunders and Michelle McPhedran for assistance during the experiments; Rosemary Cicione for software coding; Rodney Millard for stimulator design; Thomas Landry and Sam John for data collection; and Sue Pierce and Elisa Borg for animal care. This work was performed at the Bionics Institute at St. Vincent's Hospital, and the Centre for Eye Research from the University of Melbourne at the Royal Victorian Eye and Ear Hospital. Funding was provided by the Ian Potter Foundation and the Australian Research Council through its Special Research Initiative in Bionic Vision Science and Technology grant to Bionic Vision Australia (BVA). The Bionics Institute and the Centre for Eye Research Australia acknowledge the support they receive from the Victorian Government through its Operational Infrastructure Support Program.

References

[1] Shepherd R K, Shivdasani M N, Nayagam D A, Williams C E and Blamey P J 2013 Visual prostheses for the blind *Trends Biotechnol* **31**(10) 562-71 Epub 2013/08/21

[2] Hartong D T, Berson E L and Dryja T P 2006 Retinitis pigmentosa *Lancet* **368** 1795-809

[3] Geruschat D R, Turano K A and Stahl J W 1998 Traditional measures of mobility performance and retinitis pigmentosa *Optom Vis Sci* **75** 525-37

[4] Marron J A and Bailey I L 1982 Visual factors and orientation-mobility performance *Am J Optom Physiol Opt* **59** 413-26

[5] Eckhorn R, et al. 2006 Visual resolution with retinal implants estimated from recordings in cat visual cortex *Vision Res* **46** 2675-90

[6] Brindley G S 1954 The site of electrical excitation of the human eye *J Physiol* **127** 189-200

[7] Humayun M S, de Juan E, Jr, Dagnelie G, Greenberg R J, Propst R H and Phillips D H 1996 Visual perception elicited by electrical stimulation of retina in blind humans *Arch Ophthalmol* **114** 40-6

[8] Rizzo J F, III, Wyatt J, Loewenstein J, Kelly S and Shire D 2003 Methods and perceptual thresholds for short-term electrical stimulation of human retina with microelectrode arrays *Invest Ophthalmol Vis Sci* **44** 5355-61

[9] Musarella M A and MacDonald I M 2011 Current concepts in the treatment of retinitis pigmentosa *Journal of Ophthalmology* **2011** Article ID 753547

[10] Caspi A, Dorn J D, McClure K H, Humayun M S, Greenberg R J and McMahon M J 2009 Feasibility study of a retinal prosthesis *Arch Ophthalmol* **127** 398-401

[11] Klauke S, Goertz M, Rein S, Hoel D, Thomas U, Eckhorn R, Bremmer F and Wachtler T 2011 Stimulation with a wireless intraocular epiretinal implant elicits visual percepts in blind human *Invest Ophthalmol Vis Sci* **52** 449-55

[12] Wilke R, et al. 2011 Spatial resolution and perception of patterns mediated by a subretinal 16-electrode array in patients blinded by hereditary retinal dystrophies *Invest Ophthalmol Vis Sci* **52** 5995-6003

[13] Humayun M, Propst R, de Juan E, Jr, McCormick K and Hickingbotham D 1994 Bipolar surface electrical stimulation of the vertebrate retina *Arch Ophthalmol* **112** 110-6

[14] Walter P and Heimann K 2000 Evoked cortical potentials after electrical stimulation of the inner retina in rabbits *Graefes Arch Clin Exp Ophthalmol* **238** 315-8

[15] Hesse L, Schanze T, Wilms M and Eger M 2000 Implantation of retina stimulation electrodes and recording of electrical stimulation responses in the visual cortex of the cat *Graefes Arch Clin Exp Ophthalmol* **238** 840-5

[16] Gekeler F, Kobuch K, Schwahn H N, Stett A, Shinoda K and Zrenner E 2004 Subretinal electrical stimulation of the rabbit retina with acutely implanted electrode arrays *Graefes Arch Clin Exp Ophthalmol* **242** 587-96

[17] Sachs H G and Gabel V P 2004 Retinal replacement - the development of microelectronic retinal prostheses - experience with subretinal implants and new aspects *Graefes Arch Clin Exp Ophthalmol* **242** 717-23

[18] Majji A B, Humayun M S, Weiland J D, Suzuki S, D'Anna S A and de Juan E, Jr 1999 Long-term histological and electrophysiological results of an inactive epiretinal electrode array implantation in dogs *Invest Ophthalmol Vis Sci* **40** 2073-81

[19] de Balthasar C, et al. 2008 Factors affecting perceptual thresholds in epiretinal prostheses *Invest Ophthalmol Vis Sci* **49** 2303-14

[20] Chowdhury V, Morley J W and Coroneo M T 2008 Development of an extraocular retinal prosthesis: evaluation of stimulation parameters in the cat *J Clin Neurosci* **15** 900-6

[21] Yamauchi Y, Franco L M, Jackson D J, Naber J F, Ziv R O, Rizzo J F, Kaplan H J and Enzmann V 2005 Comparison of electrically evoked cortical potential thresholds generated with subretinal or suprachoroidal placement of a microelectrode array in the rabbit *J Neural Eng* **2** S48-56

[22] Nakauchi K, et al. 2005 Transretinal electrical stimulation by an intrascleral multichannel electrode array in rabbit eyes *Graefes Arch Clin Exp Ophthalmol* **243** 169-74

[23] Fujikado T, et al. 2007 Evaluation of phosphenes elicited by extraocular stimulation in normals and by suprachoroidal-transretinal stimulation in patients with retinitis pigmentosa *Graefes Arch Clin Exp Ophthalmol* **245** 1411-9
[24] Wong Y T, Chen S C, Seo J M, Morley J W, Lovell N H and Suaning G J 2009 Focal activation of the feline retina via a suprachoroidal electrode array *Vision Res* **49** 825-33
[25] Villalobos J, Allen P J, McCombe M F, Ulaganathan M, Zamir E, Ng D C, Shepherd R K and Williams C E 2012 Development of a surgical approach for a wide-view suprachoroidal retinal prosthesis: evaluation of implantation trauma *Graefes Arch Clin Exp Ophthalmol* **250** 399-407
[26] Seo J M, Kim S J, Chung H, Kim E T, Yu H G and Yu Y S 2004 Biocompatibility of polyimide microelectrode array for retinal stimulation *Mater Sci Eng C* **24** 185-89
[27] Morimoto T, et al. 2011 Chronic implantation of newly developed suprachoroidal-transretinal stimulation prosthesis in dogs *Invest Ophthalmol Vis Sci* **52** 6785-92
[28] Villalobos J, et al. 2013 A wide-field suprachoroidal retinal prosthesis is stable and well tolerated following chronic implantation *Invest Ophthalmol Vis Sci* in press
[29] Dacey D M and Petersen M R 1992 Dendritic field size and morphology of midget and parasol ganglion cells of the human retina *Proc Natl Acad Sci USA*) ed) pp 9666-70
[30] Vakkur G J and Bishop P O 1963 The schematic eye in the cat *Vision Res* **3** 357-81
[31] Greenwald S H, Horsager A, Humayun M S, Greenberg R J, McMahon M J and Fine I 2009 Brightness as a function of current amplitude in human retinal electrical stimulation *Invest Ophthalmol Vis Sci* **50** 5017-25
[32] Rizzo J F, III, Wyatt J, Loewenstein J, Kelly S and Shire D 2003 Perceptual efficacy of electrical stimulation of human retina with a microelectrode array during short-term surgical trials *Invest Ophthalmol Vis Sci* **44** 5362-69
[33] Shah H A, Montezuma S R and Rizzo J F, III 2006 *In vivo* electrical stimulation of rabbit retina: effect of stimulus duration and electrical field orientation *Exp Eye Res* **83** 247-54
[34] Shivdasani M N, et al. 2010 Evaluation of stimulus parameters and electrode geometry for an effective suprachoroidal retinal prosthesis *J Neural Eng* **7** 036008
[35] Ohta J, et al. 2007 Laboratory investigation of microelectronics-based stimulators for large-scale suprachoroidal transretinal stimulation (STS) *J Neural Eng* **4** S85-S91
[36] Fallon J B, Irvine D R F and Shepherd R K 2009 Cochlear implant use following neonatal deafness influences the cochleotopic organization of the primary auditory cortex in cats *J Comp Neurol* **512** 101-14
[37] Jensen R J and Rizzo J F, III 2007 Responses of ganglion cells to repetitive electrical stimulation of the retina *J Neural Eng* **4** S1-S6
[38] Brummer S B and Turner M J 1977 Electrical stimulation with Pt electrodes: II-Estimation of maximum surface redox (theoretical non-gassing) limits *IEEE T Bio-Med Eng* **24** 440-3
[39] John S E, Shivdasani M N, Leuenberger J, Fallon J B, Shepherd R K, Millard R E, Rathbone G D and Williams C E 2011 An automated system for rapid evaluation of high-density electrode arrays in neural prostheses *J Neural Eng* **8** 036011
[40] Cogan S F 2008 Neural stimulation and recording electrodes *Annu Rev Biomed Eng* **10** 275-309
[41] Newbold C, Richardson R, Millard R, Seligman P, Cowan R and Shepherd R 2011 Electrical stimulation causes rapid changes in electrode impedance of cell-covered electrodes *J Neural Eng* **8** 036029
[42] Tusa R J, Palmer L A and Rosenquist A C 1978 The retinotopic organization of area 17 (striate cortex) in the cat *J Comp Neurol* **177** 213-36
[43] Elfar S D, Cottaris N P, Iezzi R and Abrams G W 2009 A cortical (V1) neurophysiological recording model for assessing the efficacy of retinal visual prosthesis *J Neurosci Meth* **180** 195-207
[44] Rousche P J and Normann R A 1998 Chronic recording capability of the Utah Intracortical Electrode Array in cat sensory cortex *J Neurosci Methods* **82** 1-15
[45] Cicione R, Shivdasani M N, Fallon J B, Luu C D, Allen P J, Rathbone G D, Shepherd R K and Williams C E 2012 Visual cortex responses to suprachoroidal electrical stimulation of the retina: effects of electrode return configuration *J Neural Eng* **9** 036009

[46] Heffer L F and Fallon J B 2008 A novel stimulus artifact removal technique for high-rate electrical stimulation *J Neurosci Meth* **170** 277-84
[47] Donaldson P E K 1987 Twenty years of neurological prosthesis-making *J Biomed Eng* **9** 291-98
[48] Kanda H, Morimoto T, Fujikado T, Tano Y, Fukuda Y and Sawai H 2004 Electrophysiological studies of the feasibility of suprachoroidal-transretinal stimulation for artificial vision in normal and RCS rats *Invest Ophthalmol Vis Sci* **45** 560-66
[49] Lee S W, Seo J M, Ha S, Kim E T, Chung H and Kim S J 2009 Development of microelectrode arrays for artificial retinal implants using liquid crystal polymers *Invest Ophthalmol Vis Sci* **50** 5859-66
[50] Schanze T, Sachs H, Wiesenack C, Brunner U and Sailer H 2006 Implantation and testing of subretinal film electrodes in domestic pigs *Exp Eye Res* **82** 332-40
[51] Rose T L and Robblee L S 1990 Electrical stimulation with Pt electrodes. VIII. Electrochemically safe charge injection limits with 0.2 ms pulses (neural application) *IEEE T Bio-Med Eng* **37** 1118-20
[52] McCreery D B, Agnew W F, Yuen T G H and Bullara L 1990 Charge density and charge per phase as cofactors in neural injury induced by electrical stimulation *IEEE T Bio-Med Eng* **37** 996-1001
[53] Stein J J, Johnson S A and Berson D M 1996 Distribution and coverage of beta cells in the cat retina *J Comp Neurol* **372** 597-617
[54] Jensen R J, Ziv O R and Rizzo J F 2005 Responses of rabbit retinal ganglion cells to electrical stimulation with an epiretinal electrode *J Neural Eng* **2** S16-S21
[55] Fried S I, Hsueh H A and Werblin F S 2006 A method for generating precise temporal patterns of retinal spiking using prosthetic stimulation *J Neurophysiol* **95** 970-8
[56] Ogden T E and Brown K T 1964 Intraretinal responses of the Cynamolgus monkey to electrical stimulation of the optic nerve and retina *J Neurophysiol* **27**(Jul) 682-705
[57] Grill W M and Mortimer J T 1994 Electrical properties of implant encapsulation tissue *Ann Biomed Eng* **22** 23-33
[58] Shepherd R K, Franz B K H G and Clark G M 1990 The biocompatibility and safety of cochlear prostheses *Cochlear Prostheses* Clark G, Tong Y C, Patrick J F (Ney York: Churchill Livingstone)
[59] Davison P F and Galbavy E J 1986 Connective tissue remodeling in corneal and scleral wounds *Invest Ophthalmol Vis Sci* **27** 1478-84
[60] Zrenner E, et al. 2011 Subretinal electronic chips allow blind patients to read letters and combine them to words *Proc R Soc B* **278** 1489-97
[61] Roessler G, et al. 2009 Implantation and explantation of a wireless epiretinal retina implant device: observations during the EPIRET3 prospective clinical trial *Invest Ophthalmol Vis Sci* **50** 3003-8